http://eprints.gla.ac.uk/120674/

Vibronic effects and destruction of exciton coherence in optical spectra of J-aggregates: a variational polaron transformation approach

E. A. Bloemsma, M. H. Silvis,[*] A. Stradomska,[†] and J. Knoester[‡]

Zernike Institute for Advanced Materials,

University of Groningen, Nijenborgh 4,

9747 AG Groningen, The Netherlands

Abstract

Using a symmetry adapted polaron transformation of the Holstein Hamiltonian, we study the interplay of electronic excitation-vibration couplings, resonance excitation transfer interactions, and temperature in the linear absorption spectra of molecular J-aggregates. Semi-analytical expressions for the spectra are derived and compared with results obtained from direct numerical diagonalization of the Hamiltonian in the two-particle basis set representation. At zero temperature, we show that our polaron transformation reproduces both the collective (exciton) and single-molecule (vibrational) optical response associated with the appropriate standard perturbation limits. Specifically, for the molecular dimer excellent agreement with the spectra from the two-particle approach for the entire range of model parameters is obtained. This is in marked contrast to commonly used polaron transformations. Upon increasing the temperature, the spectra show a transition from the collective to the individual molecular features, which results from the thermal destruction of the exciton coherence.

[*] Current address: Johann Bernoulli Institute for Mathematics and Computer Science, University of Groningen, Nijenborgh 9, 9747 AG Groningen, The Netherlands

[†] Current address: School of Chemistry, University of Glasgow, Joseph Black Building, G12 8QQ Glasgow, Scotland, UK

[‡] To whom corresponce should be addressed: j.knoester@rug.nl

I. INTRODUCTION

Low-dimensional aggregates conceived by self-assembly of individual molecules in solution are of significant interest for nanoscale functional materials [1–3]. Examples of such systems include the natural light-harvesting complexes of chlorophyll molecules that appear in photosynthetic bacteria and plants [4–8], as well as aggregates formed by synthetic dye molecules, such as the well-known class of J-aggregates formed by cyanine molecules [3, 9–12]. The strong resonance interactions between the aggregated molecules in these systems give rise to charge-neutral, collective electronic excitations called Frenkel excitons [13, 14]. These excitons give rise to collective effects in the optical response, such as exchange narrowing of optical line shapes [15, 16], enhanced spontaneous emission (exciton superradiance) [17], strong nonlinear susceptibilities [18–21], and highly efficient excitation energy transfer [22–25].

Of course, in general, Frenkel excitons are not coherently spread over the entire aggregate, because their scattering on static disorder and dynamic (thermal) excitations, such as vibrations, limits their delocalization and coherence size [26–33]. The complicated interplay between intermolecular excitation transfer interactions, disorder, and coupling to vibrations and its effect on spectral and energy transport properties have been topics continuously attracting attention throughout the history of research on molecular aggregates [34, 35]. Historic examples are the formation of vibronic excitations and corresponding spectral bands and dynamics [36–40], as well as the destruction of exciton superradiance with rising temperature [17, 41]. A well-known recent example concerns the coherence of excitons in light-harvesting antenna complexes, such as FMO, and its contribution to the excitation transport efficiency in these systems [42–51]. Another recent example of interest relates to the coherence between electronic excitations on inner and outer walls of double-walled cylindrical molecular aggregates [52–57].

In this paper, we focus on the interplay between exciton-vibration coupling, intermolecular interactions, and thermal effects (dynamic disorder) in the linear optical absorption spectra of J-aggregates. We aim for an approach that allows to close the gap between various perturbative regimes, such as the weak and strong exciton-vibration coupling limits. Thus, we aim for a method that treats the intermolecular excitation transfer interactions and the interactions with the dynamic environment (vibration-excitation coupling) on equal footing,

i.e., non-perturbatively. Several numerical methods exist that go beyond the standard perturbation approaches, among which are density matrix renormalization group methods [58], multiconfiguration time-dependent Hartree methods (MCTDH) [59], hierarchical equations of motion techniques [60, 61], stochastic path integral evaluations [62], and multi-particle basis set approaches [63–66]. While these methods have clear advantages in the sense that they explore a larger part of the parameter space than the ordinary perturbation treatments, they typically require high computational costs, especially for larger aggregate sizes. Also, their complexity and the lack of analytical results makes these methods typically less insightful than perturbation treatments.

An alternative approach utilizes the polaron transformation [67–70]. This approximate method is based upon a Lang-Firsov transformation of the model Hamiltonian [71], which leads to new exciton-vibration coupling terms that remain small over a larger range of parameters than the original vibronic interaction terms. Indeed, recently, it has been shown that this method can capture both the coherent energy transfer limit and the incoherent Förster limit in a consistent way [72–76]. In these studies, the focus has been on analyzing energy transport within and between multi-chromophoric systems, while a detailed investigation of their spectroscopic features based on these polaron transformation methods has remained relatively unexplored.

Here we study the linear optical absorption spectra of J-aggregate model systems described by the Holstein Hamiltonian [67]. This model Hamiltonian is well known and has been used successfully to describe the optical spectroscopy of a variety of low-dimensional molecular aggregates [36, 37, 39]. We employ a symmetry adapted polaron transformation approach (abbreviated as APTA), which exploits the symmetry of the Hamiltonian [77, 78]. Specifically, it consists of two simultaneous transformations: a classical (full) polaron transformation which is applied to the totally symmetric collective vibrational mode, followed by a variational (partial) polaron transformation to minimize the couplings between the electronic excitations and the remaining non-symmetric collective vibrational modes. The semi-analytical expressions obtained for the low-temperature absorption spectra are compared with results obtained from direct numerical diagonalization of the model Hamiltonian in the two-particle approximation (abbreviated as TPA) [63–66], where the latter serves as a benchmark to determine the range of validity of these expressions.

We establish that using the APTA, the spectral properties associated with both of the

standard perturbation limits (weak and strong exciton-vibration coupling) are recovered, while also in between these limits the spectra give reasonably good to excellent (depending on the aggregate size) agreement with the results obtained from the TPA. In this respect, we find that the collective representation of the molecular vibrations combined with the variational nature of the polaron parameter plays a key role for the accuracy of the results in this intermediate regime. In addition, we show that higher temperatures in general destroy the spatial coherence of the excitons and their related optical features, such as the superradiant optical transition.

This paper is organized as follows. In Sec. II, we introduce the Holstein Hamiltonian model, present the symmetry adapted polaron transformation approach, and derive the expressions for the linear absorption spectrum of the molecular aggregate. In Sec. III, we give the analytical results for the spectrum at zero temperature and show explicitly how these contain both well-known perturbation limits. Section IV is devoted to the numerical results; here, we show the comparison of our method to the two-particle approximation, discuss the results in the light of related polaron transformation methods, and present the temperature dependence of the spectra. We conclude and make some final remarks in Sec. V.

II. THEORETICAL FRAMEWORK

A. Model Hamiltonian

We consider the Holstein model to describe the optical properties of an aggregate of molecules, each of which has one electronic transition that is coupled to a local vibration. The well-known corresponding Hamiltonian has the form ($\hbar = 1$) [67]

$$H = \left(E_0 + \lambda^2 \omega_0\right) \sum_n b_n^\dagger b_n + {\sum_{n,m}}' J_{nm} b_n^\dagger b_m + \lambda \omega_0 \sum_n \left(a_n + a_n^\dagger\right) b_n^\dagger b_n + \omega_0 \sum_n a_n^\dagger a_n. \quad (1)$$

Here, E_0 and ω_0 denote, respectively, the bare (adiabatic) electronic molecular transition energy and vibrational mode frequency, J_{nm} is the matrix element of the excitation transfer interaction between molecules n and m (the prime on the summation excludes the case $n = m$), and λ^2 is the dimensionless Huang-Rhys factor, which determines the coupling strength between the vibrational and electronic excitations. As we will not account for electronic disorder, all molecular transition energies E_0 are taken identical. Similarly, we do

not consider disorder in the intermolecular interactions J_{nm}. These simplifications are not restrictive, in the sense that in principle the symmetry adapted approach can be extended to Hamiltonians that include heterogeneity in the electronic site energies and couplings (see Sec. V). Furthermore, we have assumed that the frequency ω_0 and coupling strength λ^2 of the vibrational mode is the same for each molecule. This is important for the application of the symmetry adapted method, as will be explained in more detail at the end of this section (below Eq. 3). Finally, for definiteness, we will restrict ourselves to linear aggregates of equidistantly spaced molecules. We note, however, that the method may equally well be applied to systems of arbitrary dimension and geometry.

The creation (annihilation) operators for electronic and vibrational excitations on molecule n are given by $b_n^\dagger$ (b_n) and $a_n^\dagger$ (a_n), respectively. They satisfy the usual (anti-)commutation relations: $\left[b_n, b_m^\dagger\right] = \delta_{nm}\left(1 - 2b_m^\dagger b_n\right)$, $b_n^\dagger b_n^\dagger = b_n b_n = 0$, and $\left[a_n, a_m^\dagger\right] = \delta_{nm}$. These relations reflect the bosonic nature of the vibrational operators, while the electronic operators are governed by Pauli commutation relations. We stress that each molecule can carry at most one electronic excitation, while the number of vibrational excitations is unlimited.

It is clear from Eq. (1) that the nature of the eigenstates of H is determined by a competition between J_{nm} and $\lambda\omega_0$ [79, 80]. If $\lambda = 0$, a Bloch transformation diagonalizes H (assuming periodic boundary conditions for the aggregate), giving rise to collective excitation waves (Frenkel excitons) and vibrations. The eigenstates of the total Hamiltonian can then be expressed as Born-Oppenheimer products of electronic and vibrational wave functions for the whole aggregate. On the other hand, if $J_{nm} = 0$, the eigenstates can be found by introducing displaced oscillator operators, yielding single-molecule excitation states. Thus, if one of these parameters (either J_{nm} or $\lambda\omega_0$) is small compared to the other, one may attempt to find the eigenstates using a perturbation scheme.

If such a procedure fails, an alternative approach is to apply a *full polaron* transformation to Eq. (1) [71]. This transformation yields vibrational modes of the molecular excited state that are undisplaced compared to the ground state modes. Consequently, a new exciton-vibration interaction term appears after the transformation, which may be treated perturbatively. A generalization of this method is the *variational polaron* transformation where the excited state vibrational mode displacements are optimized using the variational polaron parameter [70]. The main advantage of this method is that it typically yields exciton-vibration interactions terms which remain of perturbative nature for a wider range

of system parameters J_{nm} and λ compared to the full polaron transformation. It turns out, however, that these conventional polaron transformation approaches lead to inadequate results for the optical response in the intermediate coupling regime (see Sec. IV B), indicating the importance of the remaining exciton-vibration interactions in this regime. A natural way to overcome this is to develop approaches which lead to further minimization of these coupling terms. Below, we will demonstrate that this can be accomplished by rewriting the Hamiltonian [Eq. (1)] in the collective vibrational mode representation, because it allows us to decouple in an exact way the totally symmetric vibrational mode from the electronic excitations by means of a full polaron transformation. A variational polaron transformation is then applied to the other collective modes in order to minimize the remaining coupling between the electronic excitations and these modes.

As mentioned above, the key point in our approach is to exploit the symmetry of the model. Thus, we introduce collective vibrational modes, defined by

$$a_q^\dagger = \frac{1}{\sqrt{N}} \sum_n \Phi_{nq} a_n^\dagger, \quad a_q = \frac{1}{\sqrt{N}} \sum_n \Phi_{nq} a_n, \tag{2}$$

where q denotes the vibrational quantum number and N is the total number of molecules in the aggregate. In what follows, we assume strictly real matrix elements Φ_{nq}, which can be obtained as the symmetric and antisymmetric combinations of the usual Bloch waves. Explicitly, for N odd we have: $\Phi_{nq=0} = 1$, $\Phi_{nq} = \sqrt{2}\cos(2\pi qn/N)$ if $q = -(N-1)/2, ..., -1$, and $\Phi_{nq} = \sqrt{2}\sin(2\pi qn/N)$ when $q = 1, ..., (N-1)/2$; for N even we find: $\Phi_{nq=0} = 1$, $\Phi_{nq=N/2} = (-1)^{n+1}$, $\Phi_{nq} = \sqrt{2}\cos(2\pi qn/N)$ if $q = -N/2+1, ..., -1$, and $\Phi_{nq} = \sqrt{2}\sin(2\pi qn/N)$ when $q = 1, ..., N/2 - 1$. In the collective vibrational mode representation H reads,

$$
\begin{aligned}
H = {}& \left(E_0 + \lambda^2\omega_0\right)\sum_n b_n^\dagger b_n + {\sum_{n,m}}' J_{nm} b_n^\dagger b_m + \frac{\lambda\omega_0}{\sqrt{N}}\left(a_0 + a_0^\dagger\right)\sum_n b_n^\dagger b_n + \omega_0 a_0^\dagger a_0 \\
& + \frac{\lambda\omega_0}{\sqrt{N}}\sum_{n,q\neq 0} \Phi_{nq}\left(a_q + a_q^\dagger\right) b_n^\dagger b_n + \omega_0 \sum_{q\neq 0} a_q^\dagger a_q,
\end{aligned}
\tag{3}
$$

where we have explicitly split the vibrational part of H into two components: one part describes the totally symmetric vibrational mode $q = 0$, while the other part contains all the other modes. The reason for this is that the totally symmetric mode is unique in the sense that the excited state displacements are identical for all molecules. Due to this feature, the vibrations of this mode can be completely decoupled from the electronic excitations by applying a full polaron transformation.

6

B. Polaron transformations

In general, the transformed Hamiltonian is defined by $\widetilde{H} = \exp\left(G\right) H \exp\left(-G\right)$, where G is the generator of the transformation. The *full polaron* transformation for the symmetric vibrational mode is governed by the generator,

$$G_F = \frac{\lambda}{\sqrt{N}} \left(a_0^\dagger - a_0 \right) \sum_n b_n^\dagger b_n, \tag{4}$$

which results, using Eq. (3), in the following form of $\widetilde{H}$,

$$\widetilde{H} = \left[E_0 + \lambda^2 \omega_0 \left(1 - \tfrac{1}{N} \right) \right] \sum_n b_n^\dagger b_n + {\sum_{n,m}}' J_{nm} b_n^\dagger b_m$$
$$+ \frac{\lambda \omega_0}{\sqrt{N}} \sum_{n,q \neq 0} \Phi_{nq} \left(a_q + a_q^\dagger \right) b_n^\dagger b_n + \omega_0 \sum_q a_q^\dagger a_q. \tag{5}$$

Above, we have chosen to express $\widetilde{H}$ in the original (untransformed) creation and annihilation operators for electronic excitations and vibrations, rather than in terms of their transformed counterparts. Comparison of Eqs. (3) and (5) shows that after the transformation, the totally symmetric mode is completely decoupled from the electronic excitations.

As explained above, the other collective vibrational modes can not, in general, be completely decoupled from the electronic excitations. Therefore, we proceed by applying a *variational polaron* transformation to these modes. The generator of this transformation is given by

$$G_V = \frac{\xi}{\sqrt{N}} \sum_n \sum_{q \neq 0} \Phi_{nq} \left(a_q^\dagger - a_q \right) b_n^\dagger b_n, \tag{6}$$

where $0 \leq \xi \leq \lambda$ denotes the variational polaron parameter, of which the optimal value can be found from free energy minimization arguments, as discussed at the end of this section. We note that the case $\xi = \lambda$ corresponds to a full polaron transformation, while $\xi = 0$ is associated with performing no transformation at all. After applying this second transformation to Eq. (5), we find

$$\widetilde{H} = \widetilde{E}_0 \sum_n b_n^\dagger b_n + {\sum_{n,m}}' \widetilde{J}_{nm} b_n^\dagger b_m + \omega_0 \sum_q a_q^\dagger a_q + \frac{\omega_0}{\sqrt{N}} \left(\lambda - \xi \right) \sum_{n,q \neq 0} \Phi_{nq} \left(a_q + a_q^\dagger \right) b_n^\dagger b_n, \tag{7}$$

where we have introduced the following renormalized molecular transition frequencies,

$$\widetilde{E}_0 = E_0 + \omega_0 \left(1 - \frac{1}{N} \right) \left(\lambda - \xi \right)^2, \tag{8}$$

and renormalized interactions,

$$\widetilde{J}_{nm} = J_{nm} \exp\left[\frac{\xi}{\sqrt{N}} \sum_{q \neq 0} (\Phi_{nq} - \Phi_{mq}) \left(a_q^\dagger - a_q\right)\right].$$ (9)

Comparison of Eqs. (3) and (7) shows that, after applying both a full polaron transformation (associated with the totally symmetric vibrational mode) and a variational one (associated with all other vibrational modes), the original linear exciton-vibration interaction term is still present (except for the totally symmetric vibrational mode) albeit its strength is lowered. In addition, a new coupling term between the electronic and vibrational excitations appears in the intermolecular interactions, i.e., Eq. (9).

In order to find the excited states of $\widetilde{H}$, we perform a perturbation expansion in both exciton-vibration coupling terms using the standard projection superoperator formalism [81]. The lowest perturbation order is given by the expectation value of the exciton-vibration coupling terms with respect to the thermal equilibrium situation of the vibrational modes q (mean field value). While the expectation value of the linear exciton-vibration coupling term is trivially equal to zero, the mean field value of the intermolecular interactions, denoted $\left\langle \widetilde{J}_{nm} \right\rangle$, is in general different from zero. Its value can be calculated explicitly, yielding [72]

$$\left\langle \widetilde{J}_{nm} \right\rangle = J_{nm} \exp\left[-\xi^2 \coth\left(\frac{\omega_0}{2k_B T}\right)\right],$$ (10)

where k_B is the Boltzmann constant and T the temperature. In the low-temperature limit $k_B T \ll \omega_0/2$, the electronic intermolecular interactions reduce to $\left\langle \widetilde{J}_{nm} \right\rangle = J_{nm} \exp\left(-\xi^2\right)$, which depends on the value of the variational polaron parameter: if $\xi \approx 0$ (appropriate when $|\lambda\omega_0| \ll |J_{nm}|$), we find $\left\langle \widetilde{J}_{nm} \right\rangle \approx J_{nm}$, while in the opposite case $\xi \approx \lambda$ (which holds if $|\lambda\omega_0| \gg |J_{nm}|$), we have $\left\langle \widetilde{J}_{nm} \right\rangle \approx J_{nm} \exp\left(-\lambda^2\right)$ which is smaller in magnitude than $|J_{nm}|$. Thus, due to exciton-vibration coupling the interactions between the molecules are effectively lowered, resulting in a narrower exciton band. A similar effect also occurs due to temperature: increasing the temperature leads to a decrease of $\left\langle \widetilde{J}_{nm} \right\rangle$, which in the high-temperature limit $k_B T \gg \omega_0/2$, approaches $\left\langle \widetilde{J}_{nm} \right\rangle \approx 0$. This phenomenon is typically referred to as *temperature-induced* narrowing of the exciton band, although strictly speaking it originates from the presence of vibrations.

By both adding and subtracting $\left\langle \widetilde{J}_{nm} \right\rangle$ from the right-hand side of Eq. (7), we may, after

rearranging the terms, cast it into the form $\widetilde{H} = \widetilde{H}_0 + \widetilde{H}_I$; the free Hamiltonian $\widetilde{H}_0$ reads

$$\widetilde{H}_0 = \widetilde{E}_0 \sum_n b_n^\dagger b_n + {\sum_{n,m}}' \left\langle \widetilde{J}_{nm} \right\rangle b_n^\dagger b_m + \omega_0 \sum_k a_q^\dagger a_q, \tag{11}$$

while the interaction Hamiltonian $\widetilde{H}_I$ has the form,

$$\widetilde{H}_I = {\sum_{n,m}}' \left(\widetilde{J}_{nm} - \left\langle \widetilde{J}_{nm} \right\rangle \right) b_n^\dagger b_m + \frac{\omega_0}{\sqrt{N}} (\lambda - \xi) \sum_{n,q\neq 0} \Phi_{nq} \left(a_q + a_q^\dagger \right) b_n^\dagger b_n. \tag{12}$$

Equations 11 and 12 constitute the final result for the transformed Holstein Hamiltonian within the APTA approach. Here $\widetilde{H}_0$ describes the average effect of the exciton-vibration coupling on the excited state properties of the original Holstein Hamiltonian, while $\widetilde{H}_I$ contains the residual exciton-vibration interaction terms. The latter depends explicitly on the value of ξ: for $\xi \approx 0$, the intermolecular interaction term (first right-hand side term of Eq. (12)) disappears, while for $\xi \approx \lambda$, the linear exciton-vibration coupling term (second right-hand side term of Eq. (12)) vanishes. These two extremes roughly coincide with, respectively, the weak exciton-vibration coupling and weak intermolecular interactions limit of H in Eq. (3).

To end this section, we note that up to now the variational polaron parameter ξ is still undetermined. As mentioned, setting $\xi = 0$ amounts to performing no transformation, while taking $\xi = \lambda$ corresponds to applying a full polaron transformation. The main idea behind the variational polaron transformation is that the value of ξ can be adjusted such that $\widetilde{H}_I$ remains small for a wide range of parameters λ, J_{nm}, and T, and consequently may be neglected (or treated perturbatively). This value of ξ may be obtained from the Bogoliubov upper bound on the free energy, which is given by [69, 70]

$$A_B = -k_B T \ln \left[\mathrm{Tr} \left\{ \exp \left(\frac{-\widetilde{H}_0}{k_B T} \right) \right\} \right], \tag{13}$$

where $\mathrm{Tr}\{...\}$ denotes the trace over all electronic and vibrational degrees of freedom. The optimized value of ξ is that for which the free energy A_B is minimal, i.e., it can be found from the solution of the self-consistency equation $dA_B/d\xi = 0$. In general, this equation can not be solved analytically and one has to resort to numerical methods in order to find ξ.

C. Linear absorption spectrum

The absorption spectrum $A(E)$ of molecular aggregates can be obtained from Fermi's Golden Rule. Neglecting numerical prefactors, it has the following form

$$A(E) = \sum_{i,f} P_i \left| \langle f | \mathbf{M} \cdot \mathbf{e} | i \rangle \right|^2 \delta(E - \omega_{fi}). \tag{14}$$

Here i and f label the initial (before absorption) and final (after absorption) states, respectively, P_i denotes the probability that initially the system resides in state i, and $\omega_{fi} \equiv \omega_f - \omega_i$ is the energy difference between final and initial states. Furthermore, $\mathbf{e}$ gives the polarization of the incident light beam, while $\mathbf{M}$ is the total dipole operator of the aggregate, which is taken as a sum of single-molecule dipole operators, $\boldsymbol{\mu}_n(b_n^\dagger + b_n)$, where $\boldsymbol{\mu}_n$ denotes the transition dipole matrix element (assumed real) of molecule n. It is clear from Eq. (14) that the calculation of $A(E)$ requires knowledge of the initial and final states. These can not, in principle, be obtained in a simple way from Eq. (1), because the exciton-vibration coupling term mixes the vibrational and electronic parts of the eigenstates. Below we will show how $A(E)$ can be obtained in a straightforward manner from $\widetilde{H}$.

In Sec. II B, we showed that the transformed Hamiltonian can be written into the form $\widetilde{H} = \widetilde{H}_0 + \widetilde{H}_I$ and discussed that the variational polaron parameter ξ can be used to minimize the transformed exciton-vibration interaction term $\widetilde{H}_I$. Henceforth, to find the eigenstates of $\widetilde{H}$, we perform a perturbation expansion in $\widetilde{H}_I$ thereby neglecting any terms of higher order than the lowest one. In this approximation, we have $\widetilde{H} = \widetilde{H}_0$ (by construction, the mean field value $\langle \widetilde{H}_I \rangle = 0$); therefore, the eigenstates of $\widetilde{H}$ are identical to those of $\widetilde{H}_0$. Because electronic excitations and vibrations are completely decoupled in $\widetilde{H}_0$ (Eq. 11), the eigenstates follow directly as products of the individual electronic and vibrational excited states of the aggregate. This allows us to evaluate them separately, as detailed below.

We first consider the electronic part of the eigenstates. They can be obtained by diagonalizing the electronic part of $\widetilde{H}_0$, i.e., the first two terms on the right-hand side of Eq. (11). This yields exciton states of the general form

$$|k\rangle = \sum_n \Psi_{nk} b_n^\dagger |g\rangle, \tag{15}$$

with corresponding energies denoted by E_k. Here k denotes the excitation quantum number and $|g\rangle$ is the electronic ground state of the aggregate (i.e., the state where all molecules

reside in their respective ground states). Explicitly, for an ordered (periodic) system, the exciton state coefficients Ψ_{nk} follow from the usual Bloch waves.

Next, we address the vibrational part of $\widetilde{H}_0$, i.e., the last term on the right-hand side of Eq. (11). Expressed in terms of the ladder operators, they are given by

$$|N_q\rangle = \frac{\left(a_q^\dagger\right)^{N_q}}{\sqrt{N_q!}}\,|0_q\rangle, \tag{16}$$

where N_q is the number of vibrational quanta of mode q and $|0_q\rangle$ denotes the lowest (ground) vibrational state of this mode, i.e., we have $a_q\,|0_q\rangle = 0$. The energy of the eigenstate $|N_q\rangle$ is given by $E_{N_q} = N_q\omega_0$.

The absorption spectrum of the molecular aggregate can now be derived from Eq. (14). When we assume that the aggregate starts in the collective electronic ground state, the initial state in Eq. (14) is given by $|i\rangle = |g\rangle \prod_q |N_q\rangle$. The final state is expressed likewise as $|f\rangle = |k\rangle \prod_q |M_q\rangle$, where the aggregate is assumed to be raised to an electronically excited state $|k\rangle$ right after absorption. Because the initial and final states are obtained from the transformed Hamiltonian $\widetilde{H}_0$, we need to transform $A(E)$ as well. Replacing the total dipole operator $\mathbf{M}$ by its transform $\widetilde{\mathbf{M}}$, we obtain the following general expression for $A(E)$

$$
\begin{aligned}
A(E) = {} & \mu^2 \sum_{k,\{N_q\},\{M_q\}} P_{\{N_q\}} \\
& \times \left| \langle M_0 | e^{\frac{\lambda}{\sqrt{N}}\left(a_0^\dagger - a_0\right)} | N_0 \rangle \sum_n \Psi_{nk} \prod_{q\neq 0} \langle M_q | e^{\frac{\xi}{\sqrt{N}}\Phi_{nq}\left(a_q^\dagger - a_q\right)} | N_q \rangle \right|^2 \\
& \times \delta\left(E - \left(E_k + E_{\{M_q\}} - E_{\{N_q\}}\right)\right).
\end{aligned}
\tag{17}
$$

Here $\{N_q\}$ ($\{M_q\}$) denotes any possible configuration of vibrational quanta of the vibrational modes for the initial (final) state, $E_{\{N_q\}}$ ($E_{\{M_q\}}$) is the energy corresponding to these configurations and $P_{\{N_q\}}$ gives the probability that a certain configuration $\{N_q\}$ occurs initially. Furthermore, we took for simplicity the single-molecule transition dipoles equal in magnitude, i.e. $|\boldsymbol{\mu}_n| = \mu$, and oriented along $\mathbf{e}$.

It follows from Eq. (17) that, in principle, transitions between all vibrational states in initial and final states are allowed; the strengths of these transitions are determined by vibrational overlap integrals $U_{NM} \equiv \langle M | \exp\left(s\left(a^\dagger - a\right)\right) | N \rangle$, explicitly given by [81]

$$U_{NM} = \exp\left(\frac{-s^2}{2}\right) \sum_{p=0}^{N} \frac{s^{M-N+p}}{(M-N+p)!} \frac{(-s)^p}{p!} \frac{\sqrt{N!M!}}{(N-p)!}. \tag{18}$$

Beside the vibrational overlap integrals, $P_{\{N_q\}}$ also has to be determined. When the vibrational states are in thermal equilibrium, $P_{\{N_q\}}$ has the form,

$$P_{\{N_q\}} = \frac{\exp\left(-E_{\{N_q\}}/kT\right)}{\sum_{\{N_q\}} \exp\left(-E_{\{N_q\}}/kT\right)},\tag{19}$$

where the denominator is introduced to guarantee that $\sum_{\{N_q\}} P_{\{N_q\}} = 1$.

III. ZERO-TEMPERATURE ABSORPTION SPECTRUM

A. General expressions

At $T = 0$, Eq. (17) is considerably simplified because initially (before absorption) only the vibrational ground states are occupied [see Eq. (19)]. Specifically, the initial state is given by $|i\rangle = |g\rangle \prod_q |N_q = 0\rangle$. As a result, the only important vibrational overlap integrals are $U_{0M} \equiv \langle M| \exp\left[s\left(a^\dagger - a\right)\right] |0\rangle$. These can be calculated using Eq. (18), yielding $U_{0M} = \exp\left(-s^2/2\right) s^M \left(M!\right)^{-1/2}$. This then leads to the following expression for $A\left(E\right)$,

$$\begin{aligned}
A\left(E\right) =& \mu^2 \exp\left(-\frac{\lambda^2}{N}\right) \exp\left(-\frac{\xi^2}{N}\left(N-1\right)\right) \sum_{k,\{M_q\}} \frac{1}{\prod_q M_q!} \left(\frac{\lambda^2}{N}\right)^{M_0} \\
& \times \left|\sum_n \Psi_{nk} \prod_{q\neq 0} \left(\frac{\xi\Phi_{nq}}{\sqrt{N}}\right)^{M_q}\right|^2 \delta\left(E - \left(E_k + \omega_0 \sum_q M_q\right)\right),
\end{aligned}\tag{20}$$

where we made use of the relation $\sum_{q\neq 0} \Phi_{nq}^2 = N - 1$ (completeness).

Equation (20) may be simplified even further by realizing that the vibronic transitions associated with each of the exciton states can be classified into manifolds according to the number of vibrational excitation quanta involved, as these transitions have the same energy. The energetically lowest manifold consists of the transitions to the vibrational ground state, which is the state where all modes are in their respective vibrational ground states ($M_q = 0$ for all q). This manifold is typically referred to as the $0-0$ vibronic band (or $0-0$ vibronic line). The second lowest manifold contains transitions to N states that carry a single vibrational quantum. This manifold is termed accordingly as the $0-1$ vibronic band and has energy equal to $E = E_k + \omega_0$ (where E_k is the energy of the kth exciton state). The next manifold, with energy equal to $E = E_k + 2\omega_0$, consists of all possible states that have two vibrational quanta, etc. The transition strength of the manifold with M vibrational

12

excited quanta together with the simultaneous excitation of the exciton state k, denoted I_{0-M}^k, is given by

$$
\begin{aligned}
I_{0-M}^k = {} & \mu^2 \exp\left(-\frac{\lambda^2}{N}\right) \exp\left(-\frac{\xi^2}{N}(N-1)\right) \\
& \times \frac{1}{M!}\left[\left(\frac{\lambda^2 + \xi^2(N-1)}{N}\right)^M + \left(\sideset{}{'}\sum_{n,m} \Psi_{nk}\Psi_{mk}\right)\left(\frac{\lambda^2 - \xi^2}{N}\right)^M\right],
\end{aligned} \tag{21}
$$

where the prime in the summation excludes the case $n = m$; the energies corresponding to these transitions are given by $E = E_k + \omega_0 M$. In deriving Eq. (21), we used the relation $\sum_{q\neq 0} \Phi_{nq}\Phi_{mq} = -1$. We note that the spectrum in terms of I_{0-M}^k is given by

$$
A(E) = \sum_{k,M} I_{0-M}^k \delta(E - (E_k + M\omega_0)). \tag{22}
$$

B.   Molecular dimer

To gain more physical insight into Eqs. (20), (21), and (22) we will discuss in this section the simplest example of an aggregate, namely the dimer, and show how these expressions give rise to the well-known zero-temperature absorption spectra in the standard perturbation limits of the Holstein Hamiltonian. For explicitness, our dimer model consists of two molecules, labeled 1 and 2, with equal transition energies E_0 (i.e., no electronic disorder) and coupled via a resonant energy transfer interaction, denoted by J (we take $J < 0$). The transition dipoles are oriented parallel to each other with equal magnitude μ and each electronic excitation is coupled to a vibrational mode of frequency ω_0 with strength λ.

From the procedure outlined in Sec. II B, it follows that $\widetilde{H}_0$ for the dimer is given by

$$
\begin{aligned}
\widetilde{H}_0 = {} & \left(E_0 + \tfrac{\omega_0}{2}(\lambda - \xi)^2\right)\left[|1\rangle\langle 1| + |2\rangle\langle 2|\right] + J\exp\left(-\xi^2\right)\left[|1\rangle\langle 2| + |2\rangle\langle 1|\right] \\
& + \omega_0\left(a_+^\dagger a_+ + a_-^\dagger a_-\right),
\end{aligned} \tag{23}
$$

where we introduced electronic excitation state vectors $|n\rangle = b_n^\dagger |g\rangle$ $(n = 1, 2)$ and included the explicit expressions for the renormalized molecular transition energy and renormalised interaction using Eqs. (8) and (10), respectively. The creation and annihilation operators for the collective symmetric $(+)$ and antisymmetric $(-)$ vibrational modes are expressed in terms of the original modes (labeled 1 and 2) as $a_\pm^\dagger = (a_1^\dagger \pm a_2^\dagger)/\sqrt{2}$ and $a_\pm = (a_1 \pm a_2)/\sqrt{2}$, respectively. The electronic part of $\widetilde{H}_0$ is a 2×2 matrix that can be diagonalized analytically,

yielding the symmetric and antisymmetric exciton states $|\pm\rangle$ and corresponding energies

$$|\pm\rangle = \frac{1}{\sqrt{2}}\left[|1\rangle \pm |2\rangle\right], \qquad E_\pm = \left(E_0 + \frac{\omega_0}{2}(\lambda - \xi)^2\right) \pm J\exp\left(-\xi^2\right). \tag{24}$$

The absorption spectrum of the molecular dimer is, using Eqs. (20) and (24), expressed as,

$$A(E) = \frac{\mu^2}{2}\exp\left(-\frac{\lambda^2 + \xi^2}{2}\right)\sum_{M_+,M_-}\frac{1}{M_+!M_-!}\left(\frac{\lambda^2}{2}\right)^{M_+}\left[\left(\frac{\xi}{\sqrt{2}}\right)^{M_-} \pm \left(\frac{-\xi}{\sqrt{2}}\right)^{M_-}\right]^2 \tag{25}$$
$$\times \delta\left(E - (E_\pm + \omega_0 M_+ + \omega_0 M_-)\right),$$

where the $\pm$ sign refers to the symmetric and antisymmetric exciton state $|\pm\rangle$, respectively. Accordingly, using Eq. (21), the transition strengths of the Mth vibrational manifold associated with excitation of one of the exciton states $|\pm\rangle$, denoted $I^\pm_{0-M}$, are given by

$$I^\pm_{0-M} = \mu^2\exp\left(-\frac{\lambda^2 + \xi^2}{2}\right)\frac{1}{M!}\left[\left(\frac{\lambda^2 + \xi^2}{2}\right)^M \pm \left(\frac{\lambda^2 - \xi^2}{2}\right)^M\right]. \tag{26}$$

Here $M = M_+ + M_-$ denotes the total number of vibrational quanta. It is evident from Eq. (26) that the total oscillator strength O, i.e., the sum of all the transition strengths, is a conserved quantity given by $O = \sum_M(I^+_{0-M} + I^-_{0-m}) = 2\mu^2$.

It follows from Eqs. (25) and (26) that the spectra strongly depend on the variational polaron parameter ξ. As explained in Sec. II B, ξ is determined by minimizing the free energy [see Eq. (13)]. For the dimer at $T = 0$, this leads to the following self-consistency equation [74],

$$\xi = \lambda\left[1 + \frac{2|J|}{\omega_0}\exp\left(-\xi^2\right)\right]^{-1}, \tag{27}$$

from which it is evident that $0 \leq \xi \leq \lambda$. In principle, the values of ξ can only be obtained by numerically solving Eq. (27). However, in the standard perturbation limits of weak and strong exciton-vibration coupling they can be approximated, respectively, by $\xi \approx 0$ and $\xi \approx \lambda$. Below, we examine these extreme limits and show that Eq. (25) correctly reproduces the optical response of the dimer in these situations.

i) $|J|/\omega_0 \ll |\lambda|$. In this limit, the exciton-vibration coupling dominates the intermolecular interaction such that the optical response is expected to be determined by the single-molecule state properties rather than by delocalized exciton states. This is consistent with Eq. (27), which in this limits yields $\xi \approx \lambda$, associated with a full polaron transformation. Setting

$\xi = \lambda$ in Eq. (25), we obtain the following approximate solution for $A(E)$,

$$A(E) \approx 2\mu^2 \exp\left(-\lambda^2\right) \sum_{M=0}^{\infty} \frac{\lambda^{2M}}{M!} \delta\left(E - E_0 - M\omega_0\right). \tag{28}$$

where we used $E_{\pm} \approx E_0$ ($|J|/\omega_0 \ll 1$) and denoted the total number of vibrational quanta by M. It follows directly from Eq. (28) that $A(E)$ is simply given by the sum of the two single-molecule spectra. It consists of several active transitions with energy separation between adjacent peaks given by ω_0, while the transition strengths depend both on λ and M. Here we can distinguish between the two limits: weak ($|\lambda| \ll 1$) and strong ($|\lambda| \gg 1$) exciton-vibration coupling. In the former limit, $A(E)$ is dominated by the $0-0$ transition ($M = 0$), located at E_0 and strength roughly equal to μ^2. In the opposite limit, $|\lambda| \gg 1$, the spectrum consists of multiple transition lines with strengths that obey the Poisson distribution. The transition with $M \approx \lambda^2$ has the highest intensity and is positioned at $E \approx E_0 + \lambda^2 \omega_0$.

ii) $0 \approx |\lambda| \ll |J|/\omega_0$. In this case, the intermolecular interaction dominates the vibronic coupling strength, resulting in a collective optical response of the dimer, and we have $\xi \approx 0$ from Eq. (27), consistent with performing no transformation as expected for this limit. Keeping only the lowest order term in λ in Eq. (25), $A(E)$ reduces to

$$A(E) \approx 2\mu^2 \delta\left(E - E_+\right), \tag{29}$$

where $E_+ \approx E_0 + J$. Equation (29) shows the characteristic optical response of a molecular dimer in the absence of exciton-vibration coupling: a single absorption peak that carries twice the single-molecular oscillator strength and is shifted towards the red ($J < 0$) or blue ($J > 0$) side of the energy spectrum compared to the single-molecule transition energy.

iii) $1 \ll |\lambda| \ll |J|/\omega_0$. Similar to the previous limit, the optical response is expected to be dominated by the formation of excitons and we may set $\xi \approx 0$ again. Contrary to the previous case, however, is that higher-order terms in λ can not be, a priori, discarded. In this case, $A(E)$ is approximately given by

$$A(E) \approx 2\mu^2 \exp\left(-\frac{\lambda^2}{2}\right) \sum_{M_+} \frac{1}{M_+!} \left(\frac{\lambda^2}{2}\right)^{M_+} \delta\left(E - E_+ - M_+\omega_0\right), \tag{30}$$

with $E_+ \approx E_0 + J$. Thus, we see from Eq. (30) that the symmetric exciton state carries all the oscillator strength while the antisymmetric exciton state is essentially an optically dark state, similar to Eq. (29). However, due to the strong exciton-vibration coupling

the oscillator strength is redistributed over various vibrational transitions, giving rise to a vibrational progression structure, similar to that for single molecules [Eq. (28)]. We note that in general the $0 - 0$ transition carries a little more than twice the single-molecule $0 - 0$ oscillator strength, while the distribution of oscillator strengths of the higher vibrational replicas also differs slightly from the sum of single-molecule transitions. These effects are related to the collective nature of the eigenstates of the dimer, resulting in a reduced effective exciton-vibration coupling strength $\lambda^* = \lambda/\sqrt{2}$.

IV. NUMERICAL RESULTS AND DISCUSSION

A. Comparison with the two-particle approximation

So far we have demonstrated that the APTA successfully reproduces the optical response of the dimer in the perturbation limits of the Holstein Hamiltonian. The important question remains whether this method is also applicable in the intermediate regime, which is inaccessible by means of the usual perturbation approaches, and how it performs for larger aggregates. To address this issue, we compare the absorption spectra obtained using the APTA with those resulting from the two-particle approximation (TPA). We stress that in case of a molecular dimer, this latter method gives numerically exact results which makes it an ideal method to test the validity of the APTA. Within the TPA, the excited states of the Hamiltonian in Eq. (1) are expressed in terms of a basis set of n-particle states. Here, an n-particle state consists of a vibronically (i.e., both vibrationally and electronically) excited molecule and $(n - 1)$ molecules that are excited vibrationally (but not electronically). Numerical diagonalization of Eq. (1) expressed in the two-particle basis state representation yields the optical spectra in a straightforward manner [63, 65, 66].

Figure 1 presents the calculated zero-temperature absorption spectra $A(E)$ of the molecular dimer for various values of J/ω_0 using the APTA (solid lines), i.e., based on Eq. (25), together with the numerical results obtained from the TPA (dashed lines). In all calculations we take $\lambda = 1$. Furthermore, here and in all other numerical results, we set $\omega_0 = 1$. To stress, however, the role of ω_0, we explicitly indicate it in parameter ratios and scales. It is clear from Fig. 1 that the spectra from both methods are almost identical to each other for a large range of values J/ω_0. Thus, the APTA captures not only the standard perturbation

16

regimes, but in fact also can successfully reproduce the optical response of the dimer in the intermediate regime. This will be discussed in more detail below.

Figure 1(a) shows $A(E)$ for $|J|/\omega_0 = 0$; here, as expected, $A(E)$ simply consists of the sum of the single-molecule spectra, clearly showing the characteristic vibrational progression of the $0 - M$ transitions for single molecules [i.e., Eq. (28)]. Note that the transition strengths of the $0 - 0$ and $0 - 1$ transition are identical for $\lambda = 1$. Increasing the intermolecular interaction to $J/\omega_0 = -0.25\lambda$, we have $A(E)$ as in Fig. 1(b). We observe that the $0 - 0$ transition strength increases slightly, while the replicas tend to lose some of their strengths. Besides these small discrepancies, $A(E)$ still resembles the single-molecule spectrum to a large extent, as expected for the weak intermolecular interaction regime.

In Figs. 1(c-e), we display $A(E)$ for the intermediate coupling regime $J/\omega_0 \approx -\lambda$. The spectra clearly start to show the optical signatures of exciton formation; that is, the absorption peaks are shifted to lower energies compared to the single-molecule case and a clear increase in the intensity of the $0 - 0$ transition (lowest energy peak) is observed. We point out that in this intermediate regime the spectra resulting from the APTA and those obtained from the TPA show somewhat larger (though still quite small) discrepancies than in the weak and strong coupling limits [Figs. 1(b) and 1(f)], mostly featured in the high-energy region of the spectra $E \geq 2\omega_0$ [Figs 1(d) and 1(e)]. This part of the spectrum is mostly dominated by vibronic transitions associated with the antisymmetric exciton state, while the low energy part is mainly determined by vibronic transitions belonging to the symmetric exciton state. We stress, however, that the overall qualitative agreement between the spectra is still very good in the intermediate coupling regime.

Finally, in Fig. 1(f) we present $A(E)$ for $J/\omega_0 = -2\lambda$, which is close to the weak exciton-vibration coupling regime. In this case, the spectrum is almost entirely determined, except for the weak absorption band seen for energies $E \approx 3\omega_0$, by the vibronic transitions connected to the symmetric exciton state, in accordance with Eq. (30). These transitions are in perfect agreement with the TPA results.

We now turn our attention to the absorption spectra for larger aggregates. To this end, we consider linear aggregates with nearest-neighbor electronic interactions J only and assume periodic boundary conditions. We will restrict ourselves to $J < 0$, as is appropriate for J-aggregates. All molecular transition dipoles have magnitude μ and identical orientation. In Fig. 2, we present the calculated zero-temperature spectra for $N = 8$ (top row) and

17

$N = 32$ (bottom row) molecules based on the APTA. These results (shown as blue solid lines) are compared with both the one (black dash-dot lines) and two (red dashed lines) particle approximation (OPA and TPA, respectively). We point out that for systems with more than two molecules, the TPA method no longer provides exact results. However, comparing the results from the OPA and the TPA does give some insight into the validity of the TPA method. In all calculations we took $\lambda = 1$. Similar to the case of the dimer, again, all the results clearly show the evolution of the spectra from the single-molecule spectrum at small values of $|J|/\omega_0$ [Figs. 2(a) and 2(d)] towards the spectrum with the characteristic exciton features [Figs. 2(c) and 2(f)] for large values of $|J|/\omega_0$.

We first consider the weak intermolecular interaction regime ($J/\omega_0 = -0.25\lambda$), depicted in Figs. 2(a) and 2(d). Here, the spectra obtained from the OPA and the TPA are almost identical, indicating that the TPA method forms a good frame of reference in this regime. Comparison of the spectra from the TPA and the APTA reveals that the number of transitions as well as their energy positions coincide reasonably well. However, the higher-energy absorption bands, arising from $0 - 1$, $0 - 2$ transitions etc., have a somewhat broader lineshape in the APTA-based spectra compared to the TPA results. The reason for this is that these bands consist of vibronic transitions associated with every exciton state. Because the exciton states have slightly different energies, this gives rise to an overall broadening of these bands. Despite this, the results obtained using the APTA are still in reasonable agreement with the TPA spectra.

Next, we increase the intermolecular interactions to $J/\omega = -\lambda$. The resulting spectra for $N = 8$ and $N = 32$ molecules in this intermediate coupling regime are displayed in Fig. 2(b) and 2(e), respectively. Similar to the dimer, we start to see exciton features where the intensity of the $0-0$ transition is increased and shifted to lower energy compared to the single-molecule spectrum. The calculated oscillator strength and spectral position of this transition roughly coincide for all three methods. On the other hand, the higher-energy structure in the spectra, associated with vibronic replicas, shows several clear differences which are most pronounced in the $N = 32$ case. In particular, in the APTA spectra the remaining oscillator strength is distributed over the entire exciton band, resulting in a long absorption tail [see Fig. 2(e)]. This stems from the fact that all non-symmetric vibrational modes are treated with the same variational parameter, such that all non-symmetric electronic eigenstates have an identical vibronic structure ($M > 0$). In contrast, the TPA method does not give rise to a

broad vibrational structure but rather yields distinct $0-1$ and $0-2$ peaks in the spectra. A possible solution to overcome this discrepancy is to describe each non-symmetric vibrational mode by its own variational parameter. In this respect, we point out that the OPA- and TPA-based spectra also deviate significantly from each other (for higher vibronic replicas), indicating that the validity of the TPA results is not clear in this region.

In Figs. 2(c) and 2(f) we present the spectra in the strong intermolecular interaction regime ($J/\omega_0 = -2\lambda$). The spectra from the APTA and the TPA are found to be in good agreement with each other. The spectra in this regime consist of the vibronic transitions (mainly $0-0$ and $0-1$) associated with the totally symmetric, lowest-energy, exciton state. In particular, we found that the ratio between the two lowest transitions is roughly equal to N/λ^2, in agreement with a weak (perturbative) exciton-vibration coupling analysis. Note also the similarity between the OPA and the TPA, which indicates that the TPA method provides trustworthy results in this region.

B. Comparison with related polaron transformations

One of the key elements of the APTA, as already explained in Sec. II, is to represent the molecular vibrational modes in terms of a set of collective modes [Eq. (2)]. This allows one to completely decouple the symmetric vibrational mode from the electronic excitations using a full polaron transformation, while the other modes are partially decoupled by means of a variational polaron transformation. In this section, we compare our results of the dimer with those obtained using a different approach in which the (variational) polaron transformation is applied directly to Eq. (1), i.e., without introducing collective modes. We distinguish between two different methods: (i) a full polaron transformation applied to both local vibrational modes (FPT method), and (ii) a variational polaron transformation for both local modes (VPT method).

Figure 3 presents the spectra calculated based on the various methods (dash-dotted lines: FPT, dashed lines: VPT, and solid lines: APTA). The results clearly reveal that in the single-molecule limit $J/\omega_0 \ll \lambda^2 = 1$ the three methods give very similar spectra [Fig. 3(a)]. The reason is that in this limit we have $\xi \approx \lambda$, which means that the transformations performed in the VPT and APTA method are very close to full polaron transformations, as performed in the FPT method. With increasing values of J/ω_0 (keeping $\lambda = 1$), we see from Figs. 3(b)

19

and 3(c) that the resulting spectra differ significantly for the different methods. In particular, for $J/\omega_0 \gg \lambda = 1$ [Fig. 3(c)], the FPT method yields an absorption structure associated with excitation of the symmetric exciton state which still looks quite similar in shape to that of the APTA method, although the energy positions of the transitions differ. The intensities of the higher vibrational replicas associated with excitation of the antisymmetric exciton state, however, are highly overestimated in the FPT method compared to the APTA. Specifically, the intensities of the higher vibrational replicas connected with the symmetric and antisymmetric exciton state are exactly the same within the FPT method. On the other hand, in the VPT method the absorption spectrum in this limit [Fig. 3(c)] consists of only the 0-0 vibronic transition associated with the symmetric exciton state, i.e., all vibrational structure is lost. The reason for this is that in this limit the variational polaron parameter is roughly equal to $\xi \approx 0$.

The above arguments suggest that in the limit of strong intermolecular interactions $J/\omega_0 \gg \lambda$ and weak exciton-vibration coupling $\lambda \ll 1$ the three methods should again give very similar results, as the effects of the higher vibrational states may to good approximation be ignored in this situation. This is illustrated in Fig. 3(d), where the absorption spectra are plotted for $\lambda^2 = 0.1$. Despite a few small discrepancies, all three methods indeed give a very similar absorption spectrum, consisting mainly of the single $0 - 0$ transition of the symmetric exciton state.

Thus, we found that in the limits $J/\omega_0 \ll \lambda$ and $1 \ll \lambda \ll J/\omega_0$, the optical response of the dimer is very similar for all polaron transformation methods, while outside these regions only the APTA yields correct absorption spectra of the dimer, as was already established through the comparison with the TPA (see Fig. 1). These results clearly demonstrate that the collective mode representation of the vibrations together with the variational nature of the polaron parameter for the antisymmetric vibrational mode are essential to correctly describe the optical response in the intermediate regime (i.e., in between the perturbation limits).

C. Thermal effects

Up till now we discussed the absorption spectra at zero temperature. In this section we address the effects of temperature on the optical spectra, again focusing on the molecular

dimer.

For temperatures $T \neq 0$, in principle any vibrational state can be occupied initially; the probability of this follows from the thermal equilibrium distribution function in Eq. (19). As a consequence, for non-zero temperatures more transitions are optically accessible, spanned over a wider range of energies compared to the $T = 0$ limit. If the linewidths of the transitions are large compared to their typical energy separation, this results in temperature-induced broadening of the lineshape. Moreover, as explained in Sec. II B, temperature also gives rise to reduction of the electronic intermolecular interactions, as can be seen from Eq. (10). Thus, we expect that with increasing temperature the spectral features associated with the coherent nature of excitons (for appropriate values of J/ω_0 and λ) diminish and, correspondingly, the optical response evolves towards the single-molecule spectra.

It is noteworthy that the value of the variational polaron parameter ξ itself also depends on temperature. For the dimer, the value of ξ follows, using Eq. (13), from the following self-consistency equation [74],

$$\xi = \lambda \left[1 + \frac{2|\langle \widetilde{J} \rangle|}{\omega_0} \coth \left(\frac{\omega_0}{2k_B T} \right) \tanh \left(\frac{|\langle \widetilde{J} \rangle|}{k_B T} \right) \right]^{-1}, \tag{31}$$

where $\langle \widetilde{J} \rangle$ is the renormalized intermolecular interaction defined in Eq. (10). For $T = 0$, the above relation reduces to Eq. (27), while in the high-temperature limit ($T \to \infty$) we find $\xi \approx \lambda$. Similar to Eq. (27), the values of ξ should, in general, be found by numerically solving the above self-consistency equation. Here we point out that with increasing temperatures, the optimal values of ξ obtained from Eq. (31) not necessarily increase towards λ in a regular fashion, as physically expected, but rather show a sudden jump towards $\xi = \lambda$ (see Ref. [69] for a detailed discussion). This also has obvious consequences for the spectral changes of the dimer with increasing temperature, as we will see below.

In Fig. 4 we show the calculated spectra of the homogeneous dimer for various values of the temperature, taking system parameters $J/\omega_0 = -\lambda$ ($\lambda = 1$). The spectra clearly reveal the destruction of the optical features associated with coherent electronic excitations with increasing temperature, as already anticipated above. For low temperatures, as plotted in Fig. 4(a) ($k_B T/\omega_0 = 0.5$), the absorption spectrum is not significantly changed compared to the zero-temperature case [see Fig. 1(d)]. The most pronounced effect of temperature here is the formation of an additional small low-energy transition, which can be associated with $1 - 0$ vibronic transitions of the symmetric exciton state. Increasing the temperature

21

to $k_B T/\omega_0 = 1$, we see from Fig. 4(b) that the intensity of this transition is increased while at the same time a new low energy transition appears (associated with $2 - 0$ transitions). While these thermal effects lead to minor redistributions of the oscillator strengths over the various transitions, the excitonic character is still preserved, as can clearly be seen through comparison with the single-molecule spectra displayed in Figs. 4(a) and 4(b).

A further increase in the temperature to $k_B T/\omega_0 = 1.5$ gives rise to a drastic change in the optical response, as seen in Fig. 4(c). In fact, at this temperature the spectrum of the dimer is identical to the sum of the single-molecule spectra; the physical explanation for this is the destruction of intermolecular coherence when $k_B T$ exceeds ω_0. Mathematically, the reason for the drastic change is that the value of the variational polaron parameter makes a sudden jump towards the value $\xi = \lambda$, as touched upon already below Eq. (31), resulting in single-molecule features. For the system parameters used here ($J/\omega_0 = -\lambda$), we found that this discontinuity (sudden jump) occurs around $k_B T/\omega_0 \approx 1.2$. Finally, if we increase the temperature even more to $k_B T/\omega_0 = 2$ we observe that the spectrum of the dimer remains similar to the sum of the single-molecule spectra, as expected. The only difference between the spectra in Figs. 4(c) and 4(d) is that for higher temperatures generally more vibrational transitions are optically active, which occur both at the low- and high-energy sides of the spectrum.

V. SUMMARY AND CONCLUDING REMARKS

We have investigated the linear optical response of molecular J-aggregates by applying a symmetry adapted polaron transformation approach (APTA) to the underlying Holstein Hamiltonian. This method is based on the symmetry of the model and consists of two polaron transformations: (i) a full transformation to completely decouple the symmetric collective vibrational mode from the electronic excitations, and (ii) a variational (partial) transformation to minimize the coupling between the electronic excitations and the remaining (non-symmetric) vibrational modes. As a result, the expressions for the absorption spectrum are expected to be valid for a wide range of exciton-vibration couplings, intermolecular interactions, and temperatures, beyond the standard perturbation limits of weak (strong) exciton-vibration (excitation transfer) interactions. To establish this, we have compared our results with those obtained from direct numerical diagonalization of the model

Hamiltonian in the two-particle basis set approximation (TPA). Although we have restricted our analysis to linear molecular aggregates, we note that the APTA approach can equally well be applied to aggregates of other dimension and geometry, as the totally symmetric vibration can always be extracted with a proper basis transformation. Similarly, in principle the method developed here is not limited to J-aggregates, but may equally well be used for H-aggregates, although in that situation the inclusion of intra-band relaxation [39, 41] will be essential to describe the optical linewidths.

It is useful to comment here on possible effects of electronic disorder, i.e. variation in the electronic molecular transition energies E and the intermolecular interactions J_{nm}. Mathematically, the symmetry-adapted polaron transformation only relies on negligible disorder in the vibrational frequency ω_0 and coupling strength λ^2. The totally symmetric vibrational mode may just as well be decoupled in the presence of electronic disorder, although it is not a priori clear how good the results then would be. Electronic disorder would lead to localization of the vibronic states on part of the aggregate, which intuitively would counteract the quality of the symmetry adapted polaron transformation approach. We have not performed an in-depth study of the effects of disorder for large aggregates, but calculations for dimers with differences in the electronic excitation energies on both molecules indicate excellent performance of the transformation for small and large values of the electronic disorder, while for intermediate values (disorder approximately equal to J) the performance still is good. It turns out that with increasing disorder the minimization of the free energy leads to an increased value of ξ, which in turn leads to a stronger reduction of the effective intermolecular interaction, thereby promoting localization.

At zero temperature, we have shown that our approach captures both the perturbation limits of weak exciton-vibration coupling, giving rise to a collective (exciton) optical response, and weak intermolecular interaction, resulting in absorption spectra with mostly single-molecule features. In between these limits, we found that our results showed reasonably good agreement with those obtained from the TPA, which strongly suggests that the APTA can also accurately describe the spectral combination of single-molecule and exciton properties associated with this intermediate regime, which in general is not accessible by means of standard perturbation techniques.

In particular, for the molecular dimer the zero-temperature spectra obtained from both methods coincided almost perfectly with each other for the entire range of model parameters.

23

With increasing number of molecules in the aggregate, the results obtained from the APTA and the TPA method started to reveal some spectral discrepancies for the intermediate regime, which were mostly manifested in the higher-energy vibronic absorption bands. The intensity and energy position of the optically relevant vibrationless transition, on the other hand, still showed good agreement between both methods. These findings reflect that using a single polaron transformation for all the non-symmetric vibrational modes is likely an oversimplification for aggregates consisting of many molecules.

We have also compared the zero-temperature spectra of the dimer with those obtained from related polaron techniques, where either a full or variational transformation is applied to both vibrational modes in the Hamiltonian. While all three approaches gave similar results for the weak exciton-vibration coupling and weak intermolecular interaction limits, only the augmented polaron scheme could successfully explain the optical response of the dimer in the intermediate regime. These results illustrate the key importance of introducing a collective mode representation of the molecular vibrations together with a polaron transformation of variational nature to minimize the remaining vibronic interactions.

With increasing temperature, the absorption spectra evolved from having collective optical properties, owing to the coherent nature of the exciton states, to the single-molecule features, associated with spatially incoherent electronic excitations (i.e., single-molecule excitations). These spectral changes originate from reduced effective intermolecular interaction strengths at higher temperatures. We note that within our APTA method, the spectral changes do not occur in a smooth, regular fashion with increasing temperature, as would physically be expected. Rather, the spectra reveal a sudden drastic change of their optical features, resulting from a discontinuity in the variational parameter. It would be worthwhile, therefore, to explore alternative ways to optimize this parameter which allows one to circumvent such discontinuities.

To end, we point out that all the results shown here were calculated on a standard, commercially available computer and took at most a calculation time in the order of minutes. This clearly demonstrates the low computational costs and implementation simplicity of the presented method. In that respect, our approach can also be extended to incorporate more complex models of the environment of the aggregate, including for example spectral densities (large number of independent vibrational modes), possible environmental correlations and non-equilibrium situations. Finally, the perturbation nature of our method allows for the

evaluation of (semi-)analytical expressions for the spectra, which often can provide deeper insight into the physics than numerical methods.

ACKNOWLEDGEMENT

[1] J.M. Lehn, Proc. Natl. Acad. Sci. **99**, 4763 (2002).

[2] G. D. Scholes and G. Rumbles, Nat. Mater. **5**, 683 (2006).

[3] F. Würthner, T. E. Kaiser, and C. R. Saha-Möller, Angew. Chem. Int. Ed. **50**, 3376 (2011).

[4] H. van Amerongen, L. Valkunas, and R. van Grondelle, *Photosynthetic Excitons* (World Scientific, Singapore, 2000).

[5] G. T. Oostergetel, M. Reus, A. Gomez Maqueo Chew, D. A. Bryant, E. J. Boekema, and A. R. Holzwarth, FEBS Lett. **581**, 5435 (2007).

[6] G. D. Scholes, G. R. Fleming, A. Olaya-Castro, and R. van Grondelle, Nat. Chem. **3**, 763 (2011).

[7] M. Jendrny, T. J. Aartsma, and J. Köhler, J. Phys. Chem. Lett. **3**, 3745 (2012).

[8] G. S. Orf and R. E. Blankenship, Photosynth. Res. **116**, 315 (2013).

[9] E. E. Jelley, Nature **138**, 1009 (1936); **139**, 631 (1937).

[10] G. Scheibe, Angew. Chem. **49**, 563 (1936); **50**, 212 (1937).

[11] J-Aggregates, vol. 2, ed. T. Kobayashi, World Scientific: Singapore, 2012.

[12] S. Kirstein and S. Daehne, International Journal of Photoenergy, vol. 2006, Article ID 20363 (2006); C. Spitz, J. Knoester, A. Ouart, and S. Daehne, Chem. Phys. **275**, 271 (2002).

[13] J. I. Frenkel, Phys Rev. **37**, 17 (1931); **37**, 1273 (1931).

[14] J. Franck and E. Teller, J. Chem. Phys. **6**, 861 (1938).

[15] E. W. Knapp, Chem. Phys. Lett. **85**, 73 (1984).

[16] J. Knoester, J. Chem. Phys. **99**, 8466 (1993).

[17] S. de Boer, K. Vink, and D. A. Wiersma, Chem. Phys. Lett. **137**, 99 (1987); S. de Boer, and D. A. Wiersma, Chem. Phys. Lett. **165**, 45 (1990); H. Fidder, J. Knoester, and D. A. Wiersma, Chem. Phys. Lett. **171**, 529 (1990).

[18] V. L. Bogdanov, E. N. Viktorova, S. V. Kulya, and A. S. Spiro, Pis'ma Zh. Eksp. Teor. Fiz. **53**, 100 (1990); JETP Lett. **53**, 105 (1991).

[19] Y. Wang, J. Opt. Soc. Am. B **8**, 981 (1991).

[20] F. C. Spano and S. Mukamel, Phys. Rev. Lett. **66**, 1197 (1991).

[21] J. Knoester, Chem. Phys. Lett. **203**, 371 (1993).

[22] V. M. Agranovich and M. D. Galanin, *Electronic Excitation Energy Transfer in Condensed Matter* (North-Holland, Amsterdam, 1982).

[23] J. Pšenčík, Y. Z. Ma, J. B. Arellano, J. Hála, and T. Gillbro, Biophys. J. **84**, 1161 (2003).

[24] C. Röger, M. G. Müller, M. Lysetka, Y. Miloslavina, A. R. Holzwarth, and F. Würthner, J. Am. Chem. Soc. **128**, 6542 (2006).

[25] A.T. Haedler, K. Kreger, A. Issac, B. Wittmann, M. Kivala, N. Hammer, J. Köhler, H.W. Schmidt, and R. Hildner, Nature **523**, 196 (2015).

[26] M. Schreiber and Y. Toyozawa, J. Phys. Soc. Jpn. **51**, 1528 (1982); **51**, 1537 (1982).

[27] H. Fidder, J. Knoester, and D. A. Wiersma, J. Chem. Phys. **95**, 7880 (1991).

[28] A.V. Malyshev and F. Domínguez-Adame, Chem. Phys. Lett. **313**, 225 (1999).

[29] C. Wu, S.V. Malinin, S. Tretiak, and V. Chernyak, Nat. Phys. **2**, 631 (2006).

[30] P. Walczak, A. Eisfeld, and J. S. Briggs, J. Chem. Phys. **128**, 044505 (2008); A. Eisfeld and J.S. Briggs, Phys. Rev. Lett. **96**, 113003 (2006).

[31] E.A. Bloemsma, S.M. Vlaming, V.A. Malyshev, and J. Knoester, Phys. Rev. Lett. **114**, 156084 (2015).

[32] F. C. Spano, Acc. Chem. Res. **43**, 429 (2010).

[33] R. Tempelaar, F.C. Spano, J. Knoester, and T.L.C. Jansen, J. Phys. Chem. Lett. **5**, 1505 (2014).

[34] P. Reineker, in *Exciton Dynamics in Molecular Crystals and Aggregates*, Vol. 94 of *Springer Tracts in Modern Physics* (Springer-Verlag, Berlin, 1982).

[35] M. Schröter et al., Phys Rep. **567**, 1 (2015).

[36] P. O. J. Scherer and S. F. Fisher, Chem. Phys. **86**, 269 (1984).

[37] L. van Dijk, S. P. Kersten, P. Jonkheijm, P. van der Schoot, and P. A. Bobbert, J. Phys. Chem. B **112**, 12386 (2008).

[38] R. L. Fulton and M. Gouterman, J. Chem. Phys **35**, 1059 (1961).

[39] A. Stradomska and J. Knoester, J. Chem. Phys. **133**, 094701 (2010); Y. Wan, A. Stradomska, S. Fong, Z. Guo, R.D. Schaller, G.P. Wiederrecht, J. Knoester, and L. Huang, J. Phys. Chem. C **118**, 24854 (2014).

[40] C. Warns, I. J. Lalov, and P. Reineker, J. Lumin. **129**, 1840 (2009).

[41] D.J. Heijs, V.A. Malyshev, and J. Knoester, Phys. Rev. Lett. **95**, 177402 (2005)

[42] A. M. Oijen, M. Ketelaars, J. Köhler, T. J. Aartsma, and J. Schmidt, Science **285**, 400 (1999); Chem. Phys. **247**, 53 (1999).

[43] T. Brixner, J. Stenger, H. M. Vaswani, M. Cho, R. E. Blankenship, and G. R. Fleming, Nature **434**, 625 (2005).

[44] G. S. Engel, T. R. Calhoun, E. L. Read, T. K. Ahn, T. Mancal, Y-C. Cheng, R. E. Blankenship, and G. R. Fleming, Nature **446**, 782 (2007).

[45] G. Panitchayangkoon, D. Hayes, K. A. Fransted, J. R. Caram, E. Harel, J. Wen, R. E. Blankenship, and G. S. Engel, Proc. Natl Acad. Sci. USA **107**, 12766 (2010).

[46] E. Collini, C. Y. Wong, K. E. Wilk, P. M. G. Curmi, P. Brumer, and G. D. Scholes, Nature **463**, 644 (2010).

[47] M. T. Milder, M. T. B. Brüggemann, R. van Grondelle, J. L. Herek, Photosynth. Res. **104**, 257 (2010).

[48] A. Ishizaki, and G. R. Fleming Ann. Rev. Cond. Mat. Phys. **3**, 333 (2012).

[49] L. Cleary and J. Cao, New J. Phys. **15**, 125030 (2013); J. M. Moix, M. Khasin, and J. Cao, New J. Phys. **15**, 085010 (2013).

[50] A. Chenu, and G. D. Scholes, Ann. Rev. Phys. Chem. **66**, 69 (2015).

[51] J. Schulze, and O. Kühn, J. Phys. Chem. B **119**, 6211 (2015).

[52] C. Didraga, A. Pugžlys, P. R. Hania, H. von Berlepsch, K. Duppen, and J. Knoester, J. Phys. Chem. B **108**, 14976 (2004).

[53] A. Pugžlys, P. R. Hania, C. Didraga, J. Knoester, and K. Duppen, Solid State Phenom. **97-98**, 201 (2004).

[54] J. Sperling, A. Nemeth, J. Hauer, D. Abramavicius, S. Mukamel, H. F. Kauffmann, and F. Milota, J. Phys. Chem. A **114**, 8179 (2010).

[55] D. Abramavicius, A. Nemeth, F. Milota, J. Sperling, S. Mukamel, and H. F. Kauffmann, Phys. Rev. Lett. **108**, 067401 (2012).

[56] D. M. Eisele, C. W. Cone, E. A. Bloemsma, S. M. Vlaming, C. G. F. van der Kwaak, R. J. Silbey, M. G. Bawendi, J. Knoester, J. P. Rabe, and D. A. Vanden Bout, Nature Chemistry **4**, 655 (2012).

[57] D.M. Eisele, D.H. Arias, X. Fu, E.A. Bloemsma, C.P. Steiner, R.A. Jensen, P. Rebentrost, H. Eisele, A. Tokmakoff, S. Lloyd, K.A. Nelson, D. Nicastro, J. Knoester, and M.G. Bawendi, Proc. Nat. Acad. Sci. (USA) **111**, E3367 (2014).

[58] J. Prior, A. W. Chin, S. F. Huelga, and M. B. Plenio, Phys. Rev. Lett. **105**, 050404 (2010).

[59] J. Seibt, T. Winkler, K. Renziehausen, V. Dehm, F. Würthner, H. D. Meyer, and V. Engel, J. Phys. Chem A **113**, 13475 (2009).

[60] A. Ishizaki and G. R. Fleming, J. Chem. Phys. **130**, 234111 (2009); Proc. Natl. Acad. Sci. U.S.A. **106**, 17255 (2009).

[61] M. Tanaka and Y. Tanimura, J. Phys. Soc. Jpn. **78**, 073802 (2009); J. Chem. Phys. **132**, 214502 (2010).

[62] J. M. Moix, J. Ma, and J. Cao, J. Chem. Phys. **142**, 094108 (2015).

[63] M. R. Philpott, J. Chem. Phys. **55**, 2039 (1971).

[64] M. Hoffmann and Z. G. Soos, Phys. Rev. B **66**, 024305 (2002).

[65] F. C. Spano, J. Chem. Phys. **116**, 5877 (2002).

[66] A. Stradomska and P. Petelenz, J. Chem. Phys. **130**, 094705 (2009).

[67] T. Holstein, Ann. Phys. **8**, 325 (1959); **8**, 343 (1959).

[68] S. Rackovsky and R. Silbey, Mol. Phys. **25**, 61 (1973).

[69] D. Yarkony and R. Silbey, J. Chem. Phys. **65**, 1042 (1976); **67**, 5818 (1977).

[70] R. Silbey and R. A. Harris, J. Chem. Phys. **80**, 2615 (1984); **83**, 1069 (1985); **93**, 7062 (1989).

[71] I. J. Lang and Yu. A. Firsov, Sov. Phys. JETP **16**, 1301 (1962).

[72] S. Jang, Y. -C. Cheng, D. R. Reichman, and J. D. Eaves, J. Chem. Phys. **129**, 101104 (2008); S. Jang, J. Chem. Phys. **131**, 164101 (2009); S. Jang, J. Chem. Phys. **135**, 034105 (2011).

[73] A. Nazir, Phys. Rev. Lett. **103**, 146404 (2009); D. P. S. McCutcheon and A. Nazir, Phys. Rev. B **83**, 165101 (2011).

[74] D. P. S. McCutcheon and A Nazir, J. Chem. Phys. **135**, 114501 (2011); A. Kolli, A. Nazir, and A. Olaya-Castro, J. Chem. Phys. **135**, 154112 (2011).

[75] C.K. Lee, J. Moix, and J. Cao, J. Chem. Phys. **142**, 164103 (2015).

[76] Y. Zhang, C. Yam, Y. Kwok, and G. Chen, J. Chem. Phys. **143**, 104112 (2015).

[77] V. A. Malyshev, Optics and Spectroscopy **84**, 195 (1998).

[78] N. Lu and S. Mukamel, J. Chem. Phys. **95**, 1588 (1991).

[79] W. T. Simpson and D. L. Peterson, J. Chem. Phys. **26**, 588 (1957).

[80] F.C. Spano, L Silvestri, P Spearman, L Raimondo, and S Tavazzi. J. Chem. Phys. **127**, 184703 (2007).

[81] V. May and O. Kühn, *Charge and Energy Transfer Dynamics in Molecular Systems* (Wiley-VCH, Weinheim, 2011).
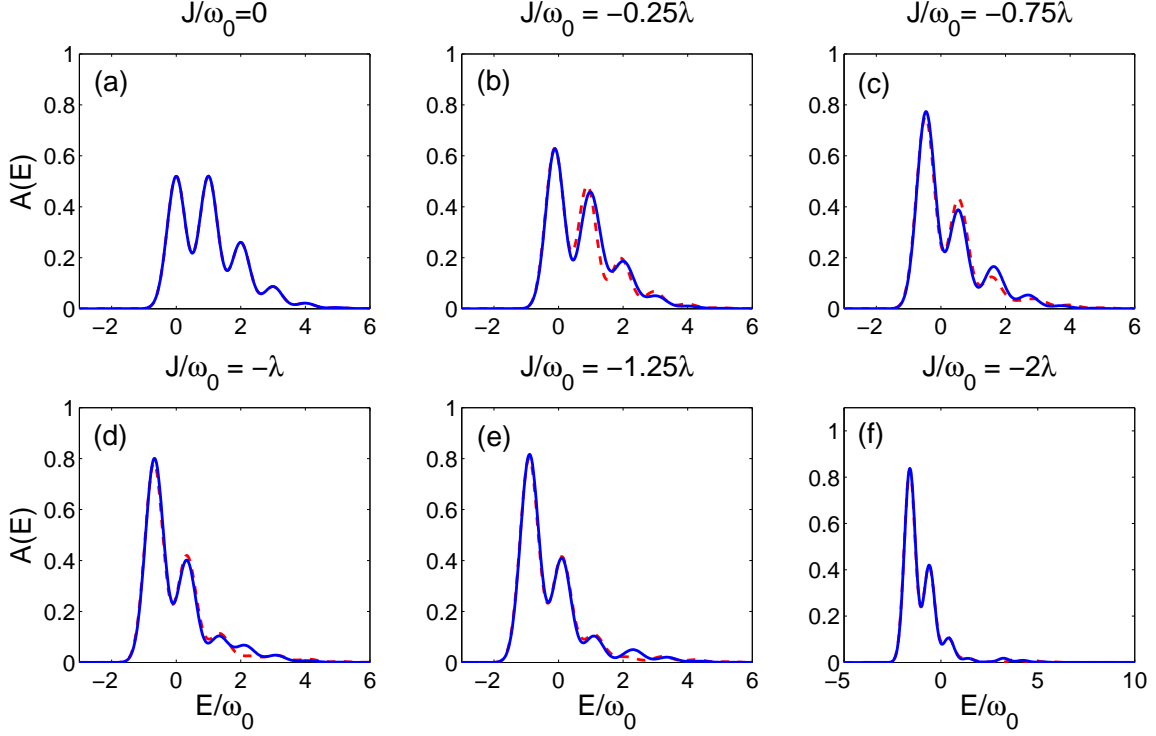
FIG. 1. Calculated zero-temperature absorption spectra for a homogeneous molecular dimer from the augmented polaron transformation approach (APTA, solid lines) and within the two-particle approximation (TPA, dashed lines). In all calculations we set $E_0 = 0$, $\mu = 1$, $\omega_0 = 1$ and take $\lambda = 1$. Values for the variational polaron parameter are: a) $\xi = 1$, b) $\xi = 0.788$, c) $\xi = 0.449$, d) $\xi = 0.363$, e) $\xi = 0.305$, f) $\xi = 0.207$. The transitions have been broadened for clarity by Gaussian functions with standard deviation given by $\Gamma = 0.28\omega_0$. The ratio of the magnitude of the intermolecular interaction and the vibrational frequency, $|J|/\omega_0$, increases from left to right and from top to bottom.
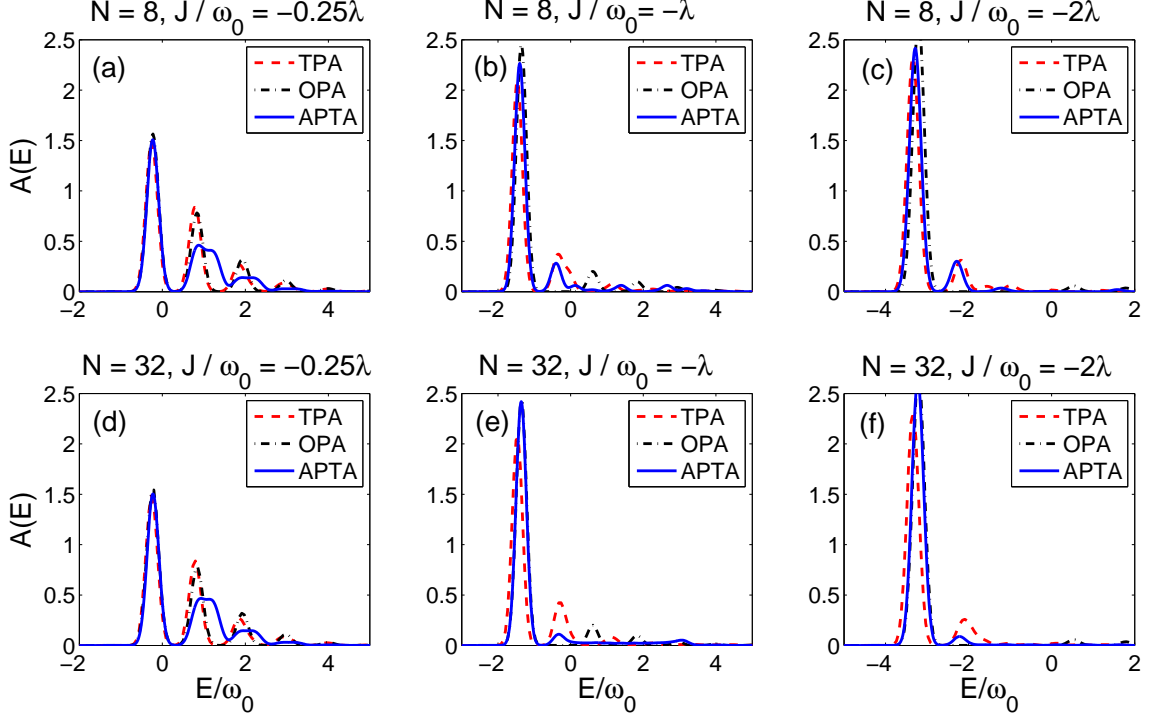
FIG. 2. Calculated zero-temperature absorption spectra for linear aggregates (using periodic boundary conditions) with $N = 8$ (top row) and $N = 32$ (bottom row) molecules and parameters similar to those in Fig. 1. Each panel shows the results based on the augmented polaron transformation approach (APTA, blue solid line), one-particle approximation (OPA, black dash-dotted line) and the two-particle approximation (TPA, red dashed line). Values for the variational polaron parameter are: a) $\xi = 0.756$, b) $\xi = 0.328$, c) $\xi = 0.185$, d) $\xi = 0.785$, e) $\xi = 0.355$, f) $\xi = 0.201$. The transitions have been broadened for clarity by Gaussian functions with standard deviation given by $\Gamma = 0.14\omega_0$. The ratio of the magnitude of the intermolecular interaction and the vibrational frequency, $|J|/\omega_0$, increases from left to right.
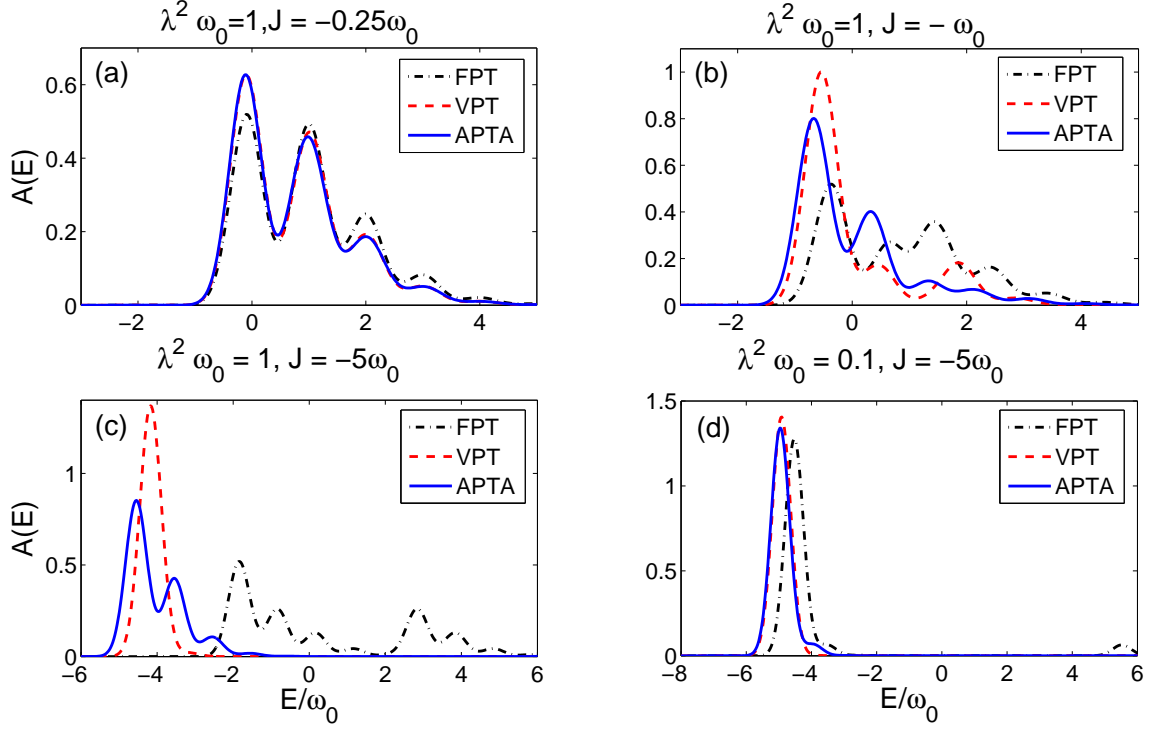
FIG. 3. Comparison of zero-temperature dimer absorption spectra obtained from the full polaron transformation method (FPT, dash-dotted lines), variational polaron transformation method (VPT, dashed lines), and augmented polaron transformation (APTA, solid lines). In all calculations we set $E_0 = 0$, $\mu = 1$, and $\omega_0 = 1$. Values for the variational polaron parameter are: a) $\xi = 0.788$, b) $\xi = 0.363$, c) $\xi = 0.092$, d) $\xi = 0.092$. The transitions have been broadened for clarity by Gaussian functions with standard deviation given by $\Gamma = 0.28\omega_0$.
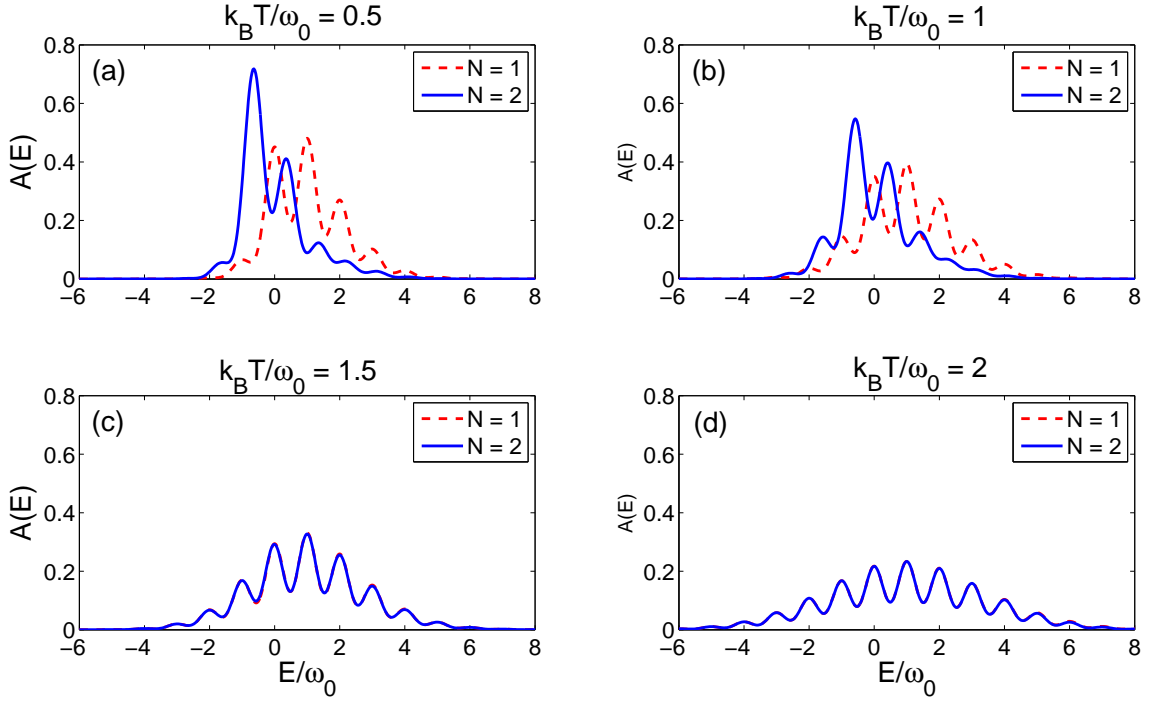
FIG. 4. Calculated temperature-dependent absorption spectra for the molecular dimer (solid lines) for system parameters $J/\omega_0 = -\lambda$. For reference, the sum of the two temperature-dependent single-molecule spectra (dashed lines) are plotted in each panel. In all calculations we set $E_0 = 0$, $\mu = 1$, $\omega_0 = 1$, and $\lambda = 1$. Values for the variational polaron parameter are: a) $\xi = 0.315$, b) $\xi = 0.288$, c) $\xi = 0.991$, d) $\xi = 0.999$. The transitions have been broadened for clarity by Gaussian functions with standard deviation given by $\Gamma = 0.28\omega_0$. The temperature increases from left to right and from top to bottom.